Published in final edited form as:
Magn Reson Med. 2009 March ; 61(3): 728–733. doi:10.1002/mrm.21876.

High-Field Diffusion MR Histology: Image-Based Correction of Eddy-Current Ghosts in Diffusion-Weighted Rapid Acquisition With Relaxation Enhancement (DW-RARE)

J. Michael Tyszka[1,*] and **Lawrence R. Frank**[2]

[1]Division of Biology, California Institute of Technology, Pasadena, California, USA

[2]Department of Radiology, University of California–San Diego, San Diego, California, USA

Abstract

High-resolution, diffusion-weighted (DW) MR microscopy is gaining increasing acceptance as a nondestructive histological tool for the study of fixed tissue samples. Spin-echo sequences are popular for high-field diffusion imaging due to their high tolerance to B_0 field inhomogeneities. Volumetric DW rapid acquisition with relaxation enhancement (DW-RARE) currently offers the best tradeoff between imaging efficiency and image quality, but is relatively sensitive to residual eddy-current effects on the echo train phase, resulting in encoding direction-dependent ghosting in the DW images. We introduce two efficient, image-based phase corrections for ghost artifact reduction in DW-RARE of fixed tissue samples, neither of which require navigator echo acquisition. Both methods rely on the phase difference in *k*-space between the unweighted reference image and a given DW image and assume a constant, per-echo phase error arising from residual eddy-current effects in the absence of sample motion. Significant qualitative and quantitative ghost artifact reductions are demonstrated for individual DW and calculated diffusion tensor images.

Keywords

diffusion weighting; magnetic resonance imaging; phase correction; RARE; magnetic resonance histology; rodent brain

Diffusion-weighted magnetic resonance imaging (DW-MRI) is well established as a noninvasive tool for exploring tissue microstructure both in vivo (1–3) and in chemically fixed samples (4). Many of the limitations imposed on DW-MRI in living systems can be dropped for fixed tissue samples, allowing increased flexibility in modifying relaxation properties (4,5), pulse sequence optimization, and reinvestment of extended imaging times by increasing spatial resolution and signal-to-noise ratio (SNR).

DW imaging sequences based on multiple spin echoes including DW Rapid Acquisition with Relaxation Enhancement (DW-RARE), are sensitive to eddy current effects on the echo

[*]Correspondence to: J. Michael Tyszka, Ph.D., 274 Beckman Institute 139-74, California Institute of Technology, 1200 E. California Blvd., Pasadena, CA 91125.

train phase. A variety of sequence modifications have been proposed that either minimize the residual eddy currents associated with diffusion preparation or moderate their effect on the refocusing pulse train. These include, but are not limited to, double-echo diffusion preparation (6), gradient crushing schemes (7), and the use of quadratic phase cycling within the refocusing pulse train (8,9). The addition of dual navigator echo acquisitions for RARE echo phase correction has also been proposed (10), but as demonstrated in this article, this approach does not in general yield an accurate estimate of the per-echo phase correction.

The use of the baseline image without diffusion weighting as a reference for eddy-current correction in DW imaging was first introduced by Haselgrove and Moore (11) and extended by Bastin (12) in the context of distortion correction for DW-EPI. In this article we apply this philosophy to *k*-space phase correction in DW-RARE and present an efficient and effective image-based ghost artifact correction algorithm primarily intended for use where eddy-current phase effects are dominant, such as for ex vivo high-resolution MR histology.

MATERIALS AND METHODS

Sample Preparation

Imaging data from a control rat brain acquired as part of an unrelated study were used to demonstrate both image-based corrections. Sample preparation was as follows: The rat was transcardiac perfusion fixed under deep anesthesia, according to a protocol approved by the Institutional Animal Care and Use Committee of the University of California, San Diego. Following fixation, the rat brain was dissected from the skull and stored in formalin for approximately 1 month. Approximately 2 weeks prior to imaging, the brain was transferred to a solution of 0.01% sodium azide in phosphate-buffered saline (PBS) to extract the formalin from the tissue. Following a week of soaking in PBS, the sample was transferred to a solution of 5 mM gadoteridol (Prohance®; Bracco Diagnostics) and 0.01% sodium azide in PBS. The sample was maintained at 4°C. Following transfer to the California Institute of Technology, the brain was stored under a perfluropolyether vacuum oil (Galden®; Solvay Solexis, Thorofare, NJ, USA) to prevent further changes in contrast enhancement prior to imaging.

Image Acquisition

All image data were acquired using an 11.7T vertical bore Avance II microimaging system (Bruker Biospin, Inc., Billerica, MA, USA) equipped with Micro 2.5 gradients capable of 150 G/cm maximum gradient strength. Fixed rat brains were secured in a custom-built Teflon holder and immersed in Galden to eliminate background signal and minimize susceptibility boundary effects (13). Samples were imaged using a 25-mm-diameter linear-mode birdcage, and sample temperature was maintained by thermostatically controlled air flow at 10°C.

A DW multishot 3D RARE pulse sequence was developed specifically for high-field diffusion MR histological applications at our facility. The Meiboom-Gill condition on the initial phase for the RARE sequence cannot be guaranteed in the presence of large diffusion-encoding gradients, a topic that has been discussed in detail elsewhere (1,9,14). Residual

eddy currents and sample motion both introduce variability in the magnetization phase at the interface between the DW and RARE sequences, leading to amplitude and phase oscillation of the subsequent Carr-Purcell-Meiboom-Gill (CPMG) echoes. The following conventions are adopted for spatial axis labeling: the frequency encoding, RARE phase-encoding, and conventional phase-encoding/slab selection dimensions are labeled *x*, *y*, and *z*, respectively.

A twofold approach to minimization of phase ghosting arising from eddy currents is employed. At the acquisition stage, both dual-echo diffusion preparation (6) and an XY-2 (9,15) phase cycling scheme were used to minimize echo amplitude oscillations in the CPMG train.

The use of a double spin echo (DSE) with variable diffusion pulse durations allows compensation for one time constant of the eddy-current decay, but cannot compensate for multiple time constants associated with different gradient axes. Since diffusion encoding engages all gradient axes, with the potential for axis-dependent and multiexponential time constants, this invariably results in only partial compensation for eddy currents. For narrower-bore high-field instruments, such as the 89-mm 11.7T magnet used in this study, the proximity of the gradient coils to cold surfaces in the magnet exacerbates these effects, making complete elimination of eddy currents at the acquisition stage extremely difficult. The remaining phase errors are removed using the retrospective, image-based corrections described below.

Imaging parameters were as follows: TR/TE_{eff} = 125 ms/14.6 ms, diffusion preparation TE = 9.4 ms, RARE echo spacing = 5.2 ms, echo train length = 8, linear RARE encoding order, second RARE echo assigned to *k*-space center, diffusion gradient pulse durations: δ_1 = 3.5 ms, δ_2 = 3.1 ms, δ_3 = 4.6 ms, δ_4 = 2.0 ms, nominal *b*-factor = 1500 s/mm^2, corrected mean *b*-factor = 2256 s/mm^2, field of view = 25.6 mm × 16.0 mm × 12.8 mm, sampled matrix = 256 × 160 × 128, sampled resolution = 100 μm isotropic, 32 DW imaging directions, four unweighted reference images, and total imaging time = 5 min 20 s per DWI.

Phase Correction

Despite the use of DSE diffusion preparation and quadratic phase cycling, image ghosts still arise from some, but not all, diffusion-encoding directions. A simple model is proposed for the origin of DW-RARE ghost artifacts in the absence of sample motion: The effect of eddy currents on the CPMG echo train is confined to the echo phase and is independent of phase-encoding gradient amplitudes, so that it is assumed constant throughout image acquisition for a given diffusion-encoding direction. The effect of the initial magnetization phase on the echo amplitudes of the classic CPMG sequence is well understood (7,9) and justifies the use of a per-echo phase correction in the absence of any other significant source of phase variation in the echo train, including sample motion.

We can assume for a stationary sample, such as fixed tissue, that the RARE image without diffusion weighting required for estimation of the apparent diffusion coefficient can also act as a phase reference for ghost correction. It follows that the phase difference between the reference and DW images can be decomposed into both intrinsic and artifactual sources as follows:

$$\Delta\phi(\mathbf{k}) = \Delta\phi_i(\mathbf{k}) + \Delta\phi_e(\mathbf{k}) + \varepsilon, \quad [1]$$

where $\Delta\varphi_i(\mathbf{k})$ is the intrinsic phase difference due to spatial variations in diffusion weighting, and $\Delta\varphi_e(\mathbf{k})$ is the per-echo phase difference due to eddy-current effects on the CPMG echo train, which is presumed constant for all phase-encoding values. The distribution of $\Delta\varphi_i(\mathbf{k}) + \varepsilon$ is assumed to have approximately zero mean, allowing robust estimates such as the sample median to isolate the per-echo phase error, $\Delta\varphi_e(\mathbf{k})$. As will be shown, this assumption holds for fixed tissue submerged in a proton-free medium, where spatial variation of the mean diffusivity is relatively homogeneous across the sample.

Two methods were explored, both based on the assumption described by Eq. [1]. The first employs a straightforward noniterative estimation scheme based upon median phase estimation. The second is an extension of the first that uses an iterative numerical optimization scheme. In the following descriptions, we define the *x*, *y*, and *z* dimensions to correspond to the frequency encoding, first (RARE) phase-encoded, and second phase-encoded dimensions of the 3D *k*-space. Both methods correct for phase errors in the RARE phase-encoding dimension (k_y) only.

The first method (median phase estimation) makes just this assumption, that the phase offset for each echo can be estimated from the median phase difference between the DW and reference *k*-space (Fig. 1). Taking the median phase across all points in *k*-space filled by a given echo from the CPMG train yields a robust estimate of the per-echo phase offset. Since the per-echo phase is most accurately determined in regions of high SNR in *k*-space, the calculation can be limited without loss of generality to a central region of a given k_x-k_z plane. We chose to use the 16 × 16 sample region in k_x-k_z centered at (k_x, k_z) = (0,0), although this kernel size can be optimized by application. The median unwrapped phase is calculated for all k_y samples assigned to a given echo number within the central k_x-k_z kernel. This median is taken as a robust estimate of the per-echo phase correction that minimizes ghosting in image space.

The second method (phase optimization) assumes, as for the median phase estimation method, that the phase offset due to eddy currents for each CPMG echo is a constant for all phase encoding values and for a given diffusion-encoding direction. We then construct a numerical optimization in which the mean square residual (MSR) signal outside the object is minimized. This signal is assumed to arise solely from Rician noise (16) and ghost artifacts arising from eddy-current effects. The phase offset for each CPMG echo is optimized by minimization of the residual signal within an external mask defined by the un-weighted reference image. This “outside” mask was constructed by thresholding the unweighted image at an intensity corresponding to the first minimum in the whole image intensity histogram greater than the noise peak. Alternatively, Otsu thresholding (17) or more sophisticated brain masking could be employed to define regions of the image containing only noise and ghost signal, though in the examples shown this was not necessary. For each iteration, all CPMG echo phases are allowed to vary without constraint, the *k*-space phase is updated accordingly, the image is reconstructed, and the cost function is calculated. As for the first method, considering only the reduced *k*-space, defined by the central k_x-k_z kernel,

and the associated image space preserves computational efficiency. Optimization was performed using an unconstrained large-scale trust region approach implemented by the Optimization Tool-box in MATLAB 2007b (The Mathworks Inc., Natick, MA, USA) with a fractional parameter and cost function convergence tolerance of 10^{-6}.

RESULTS AND DISCUSSION

Reference volumes acquired without diffusion weighting show negligible ghost artifacts using the dual-echo prepared, XY-2 phase cycling RARE sequence. The free parameter δ_4 in the DSE method used to minimize the error for a given eddy-current decay time was found empirically to be 2 ms by minimizing ghost artifacts for DW images in most, but not all, of the encoding directions. We must assume that even with calibrated gradient preemphasis, multiple eddy-current time constants are present in the form of either multiexponential decays on a given axis or different time constants for each axis. Consequently, there are insufficient degrees of freedom to completely null eddy-current effects on the initial phase of the CPMG echo train, resulting in residual phase ghosting.

The phase difference between the reference *k*-space without diffusion weighting and a given DW image displays a background phase offset associated with each echo of the CPMG train. For this sequence implementation, the CPMG echoes fill *k*-space in a linear-linear ordering, although there is no implicit limitation on the use of other ordering schemes (18). The phase difference was unwrapped using a region-growing approach described else-where (19), allowing for more accurate estimation of the background phase offset, particularly in low-SNR regions of *k*-space (Fig. 1f and 1h).

MSR signal across the “outside” mask is significantly improved by both median phase estimation and phase optimization (Figs. 2 and 3). Optimization produces a significant improvement in MSR over median phase estimation ($P = 0.023$, paired one-tailed *t*-test, degrees of freedom [df] = 31). No significant difference is observed in MSR for random or median estimated phase initialization ($P = 0.239$, paired two-tailed *t*-test, df = 31). Approximately 22% of the MSR can be assigned to phase ghost signal for the outside mask and data used here, though this fraction will vary with SNR and residual eddy-current amplitude. The optimization therefore appears to be robust to initial parameters, and a global minimum is identified in each case. This suggests that per-echo phase optimization does not require phase unwrapping of $\Delta\varphi$ and can be performed “blind.” The mean number of iterations to convergence is slightly lower when the optimization is initialized with median estimated per-echo phase corrections, as opposed to random phase correction, but not significantly at this sample size (66.8 ± 3.9 for estimated initial phases vs. 74.8 ± 2.8 for random initial phases, $P = 0.053$, paired one-tailed *t*-test, df = 31).

Calculation of the effective diffusion tensor from the high angular resolution diffusion imaging (HARDI) data was also improved by per-echo phase correction (Fig. 4). Regions of anomalously high or low fractional anisotropy (FA) were observed in a variety of locations in the uncorrected data, typically at white matter interfaces in the external capsule, midbrain, and cerebellum. Orientation anomalies were also observed, most notably in the external capsule, but presumably exist throughout the white matter.

Diffusion weighting produces an intrinsic phase difference between the respective unweighted reference and DW *k*-spaces. For the corrections described here, we assumed that these intrinsic differences were close to zero mean and median for the *k*-space regions associated with a given echo (Eq. [1]). For samples with little spatial variation in mean diffusivity, such as the fixed brain described above, the impact of diffusion weighting on the *k*-space phase is likely to meet this assumption. However, for samples that contain significant mean diffusivity variation (e.g., fixed tissue suspended in saline) or have large, internal fluid-filled spaces, this assumption may break down. The impact of CSF on eddy-current distortion corrections for DW-EPI has shown to be significant (12), suggesting that appropriate fluid suppression or modifications to the phase correction model may be required where spatial variation of diffusivity is high. We do expect the optimization approach to be less sensitive to this effect than the median estimate approach, since it can potentially be performed using the DW image alone, where, presumably, free fluid will be heavily attenuated.

The phase correction scheme described here would not be effective in the presence of significant sample motion, which is unavoidable when imaging in vivo. For application to high-field, high-resolution HARDI of fixed tissue samples, however, the method is appropriate, computationally efficient, and relatively robust. Maintaining a high SNR in white matter is a key requirement for accurate tractography and multiple-fiber modeling (20). At lower field strengths and for sample preparations that preserve longer T_2 relaxation times, the impact of DSE preparation on SNR is less significant. At high fields (7T and greater) the T_2 relaxation time for fixed brain tissue can be very short, particularly in contrast-enhanced myelinated white matter, with typical T_2 relaxation times in the range of 10–20 ms at 11.7T (4). The image-based phase corrections demonstrated here may be sufficiently robust to allow the use of single-echo (as opposed to double-echo) diffusion preparation, sacrificing eddy-current minimization at the time of acquisition for shorter TEs in order to increase white-matter SNR.

CONCLUSIONS

A phase correction scheme for eddy-current ghost minimization in DW-RARE has been implemented and tested for specific application in high-field diffusion MR histology. Uncompensated eddy-current effects on the initial phase of the CPMG echo train can be effectively removed using a per-echo phase correction, which is assumed to be constant for all phase-encoding steps for a given diffusion-encoding direction. Results in fixed rat brain demonstrate a significant reduction in ghosting artifacts with both median phase-estimated and optimized phase corrections. The algorithm is computationally efficient and straightforward to implement.

Acknowledgments

Grant sponsor: National Institutes of Health; Grant numbers: 5 R01 MH64729-05; 5 R01 MH075870-02; Grant sponsor: National Science Foundation; Grant number: DBI 0552396.

References

1. Brockstedt S, Thomsen C, Wirestam R, Holtas S, Stahlberg F. Quantitative diffusion coefficient maps using fast spin-echo MRI. Magn Reson Imaging. 1998; 16:877–886. [PubMed: 9814769]
2. Frank LR. Characterization of anisotropy in high angular resolution diffusion-weighted MRI. Magn Reson Med. 2002; 47:1083–1099. [PubMed: 12111955]
3. Tuch DS, Reese TG, Wiegell MR, Wedeen VJ. Diffusion MRI of complex neural architecture. Neuron. 2003; 40:885–895. [PubMed: 14659088]
4. Tyszka JM, Readhead C, Bearer EL, Pautler RG, Jacobs RE. Statistical diffusion tensor histology reveals regional dysmyelination effects in the shiverer mouse mutant. Neuroimage. 2006; 29:1058–1065. [PubMed: 16213163]
5. D'Arceuil HE, Westmoreland S, de Crespigny AJ. An approach to high resolution diffusion tensor imaging in fixed primate brain. Neuroimage. 2007; 35:553–565. [PubMed: 17292630]
6. Reese TG, Heid O, Weisskoff RM, Wedeen VJ. Reduction of eddy-current-induced distortion in diffusion MRI using a twice-refocused spin echo. Magn Reson Med. 2003; 49:177–182. [PubMed: 12509835]
7. Alsop DC. Phase insensitive preparation of single-shot RARE: application to diffusion imaging in humans. Magn Reson Med. 1997; 38:527–533. [PubMed: 9324317]
8. Leroux P, Hinks RS. Stabilization of echo amplitudes in FSE sequences. Magn Reson Med. 1993; 30:183–190. [PubMed: 8366799]
9. Pipe JG, Farthing VG, Forbes KP. Multishot diffusion-weighted FSE using PROPELLER MRI. Magn Reson Med. 2002; 47:42–52. [PubMed: 11754441]
10. Mori S, van Zijl PC. A motion correction scheme by twin-echo navigation for diffusion-weighted magnetic resonance imaging with multiple RF echo acquisition. Magn Reson Med. 1998; 40:511–516. [PubMed: 9771567]
11. Haselgrove JC, Moore JR. Correction for distortion of echo-planar images used to calculate the apparent diffusion coefficient. Magn Reson Med. 1996; 36:960–964. [PubMed: 8946363]
12. Bastin ME. Correction of eddy current-induced artefacts in diffusion tensor imaging using iterative cross-correlation. Magn Reson Imaging. 1999; 17:1011–1024. [PubMed: 10463652]
13. Jacobs RE, Ahrens ET, Meade TJ, Fraser SE. Looking deeper into vertebrate development. Trends Cell Biol. 1999; 9:73–76. [PubMed: 10087623]
14. Wang FN, Huang TY, Lin FH, Chuang TC, Chen NK, Chung HW, Chen CY, Kwong KK. PROPELLER EPI: an MRI technique suitable for diffusion tensor imaging at high field strength with reduced geometric distortions. Magn Reson Med. 2005; 54:1232–1240. [PubMed: 16206142]
15. Gullion T, Baker DB, Conradi MS. New, compensated Carr-Purcell sequences. J Magn Reson. 1990; 89:479–484.
16. Gudbjartsson H, Patz S. The Rician distribution of noisy MRI data. Magn Reson Med. 1995; 34:910–914. [PubMed: 8598820]
17. Otsu N. Threshold selection method from gray-level histograms. IEEE Trans Syst Man Cybernet. 1979; 9:62–66.
18. Mulkern RV, Wong ST, Winalski C, Jolesz FA. Contrast manipulation and artifact assessment of 2D and 3D RARE sequences. Magn Reson Imaging. 1990; 8:557–566. [PubMed: 2082125]
19. Tyszka JM, Mamelak AN. Quantification of B-0 homogeneity variation with head pitch by registered three-dimensional field mapping. J Magn Reson. 2002; 159:213–218. [PubMed: 12482702]
20. Behrens TE, Berg HJ, Jbabdi S, Rushworth MF, Woolrich MW. Probabilistic diffusion tractography with multiple fibre orientations: what can we gain? Neuroimage. 2007; 34:144–155. [PubMed: 17070705]

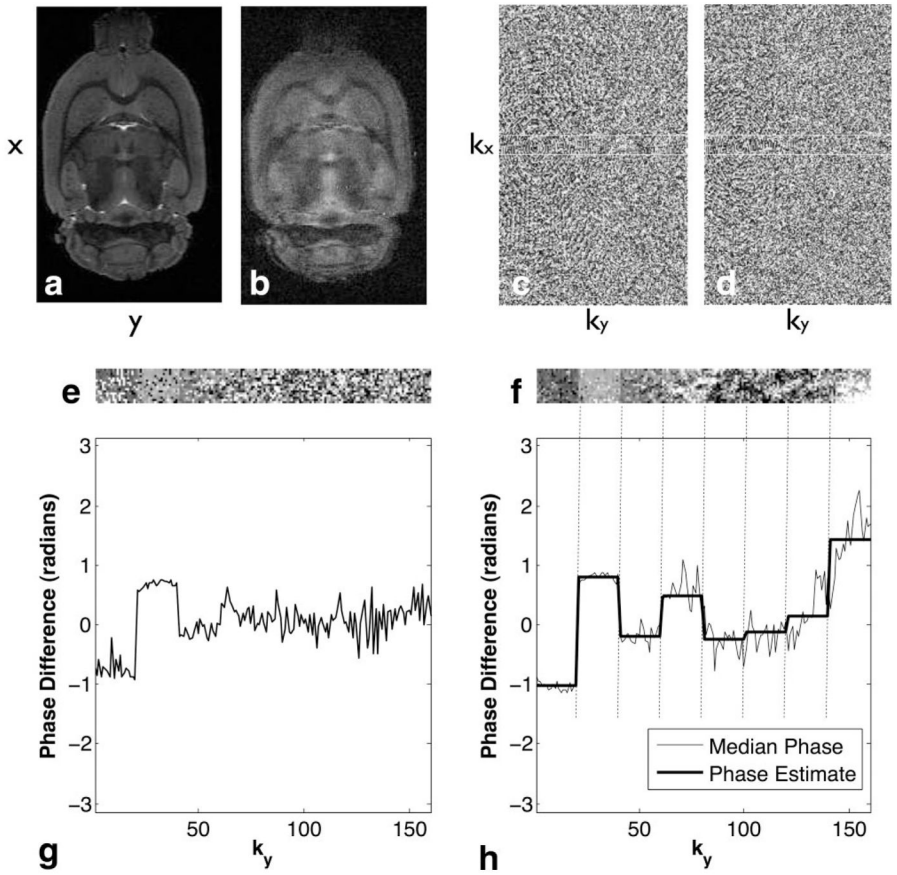

FIG. 1.

Example per-echo phase error estimation. The unweighted reference image (**a**) and a representative DW image (**b**) demonstrate the nature of the ghost artifacts arising from eddy-current phase effects on the RARE echo train. The phase angle (shown for the k_x-k_y plane at $k_z = 0$) in the corresponding reference (**c**) and DW *k*-space (**d**) shows no identifiable per-echo phase structure. For computational efficiency, phase error estimation is performed within a central reduced *k*-space (white box in c and d; see Materials and Methods, Phase Correction, for details). The phase difference (**e**) between the un-weighted and weighted reduced *k*-spaces reveals the per-echo phase offset. 3D phase unwrapping further highlights the per-echo phase offset (**f**). The median phase within the k_x-k_z kernel as a function of k_y yields an estimate of the underlying phase error (**g**). The median unwrapped phase (**h**) provides a more robust estimate of the phase error. Taking a second median across all k_y locations corresponding to a given CPMG echo yields the constant phase correction estimate (solid bold line) replicated in k_x and k_z for deghosting.

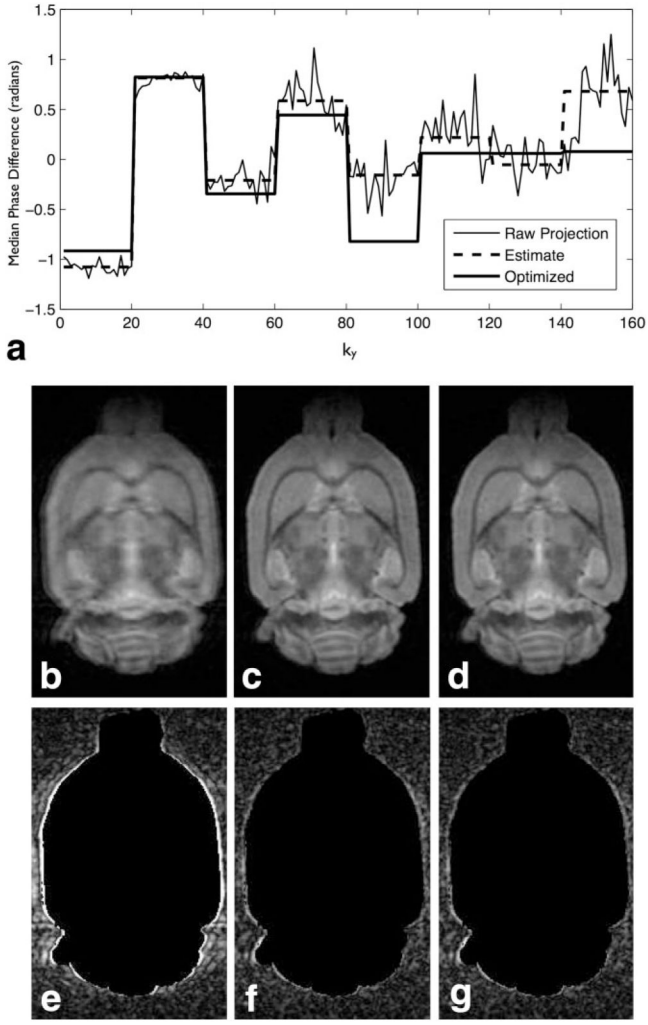

FIG. 2.

Comparison of estimated and optimized per-echo phase correction for DW-RARE histology. The optimized phase correction deviates increasingly from the median phase estimate as the local SNR in *k*-space decreases (**a**). The uncorrected (**b**,**e**), estimated (**c**,**f**), and optimized (**d**,**g**) corrected images demonstrate little subjective difference between the two ghost corrections. Applying an outside mask generated at full resolution using the same thresholding described in the text reveals the extent of ghost artifacts in the uncorrected image (e) and confirms the equivalence of the phase estimation and optimization corrections in terms of reducing background ghost amplitude outside the sample volume (f,g). A one-voxel radius Gaussian smoothing filter has been applied to these images.

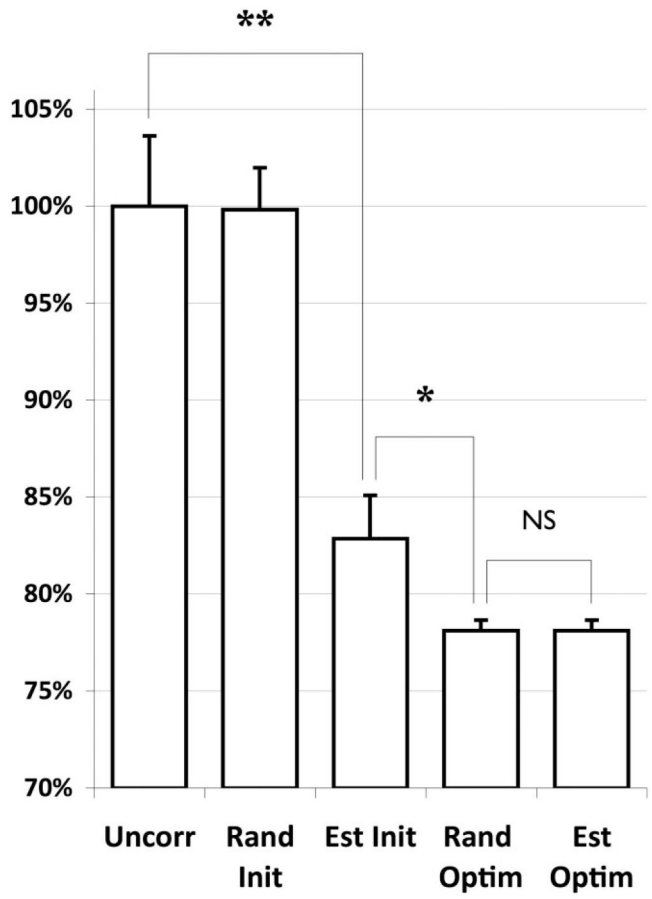

FIG. 3.

Comparison of the MSR within the outside mask for the uncorrected (Uncorr), random initial per-echo phase (Rand Init), median phase estimated initial phase (Est Init), optimized phase from random initialization (Rand Optim), and optimized phase from estimated initialization (Est Optim). All residuals are normalized to the mean uncorrected residual and expressed as a percentage. The mean residuals are calculated over all DW images in the series ($N = 32$). Error bars are standard error of the mean. Median phase estimation results in a highly significant reduction in MSR compared to no correction (*). Optimization in turn produces a significant improvement over median estimation alone (**) but there is no significant difference (NS) in final MSR between the initialization approaches.

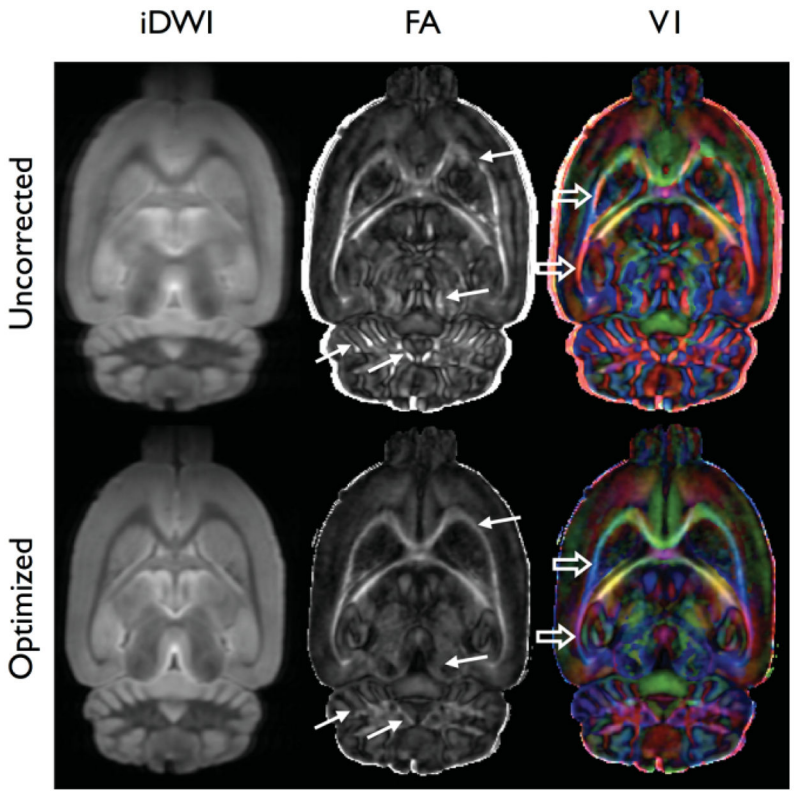

FIG. 4.

Comparison of corrected and uncorrected diffusion tensor results. The isotropic DW image (iDWI), FA, and principal eigenvectors (V1) were calculated from 3D DW-RARE HARDI data (32 DW and four unweighted images). Ghosting in individual DWIs results in an effective blurring of the iDWI. Anomalous regions of high anisotropy in the FA map (solid arrows) and incorrect eigenvector orientation in the directional-coded, FA-weighted V1 data (open arrows) are apparent. A one-voxel radius Gaussian smoothing filter has been applied to the original HARDI data.